Journal of Applied Electrochemistry **32**: 91–95, 2002.

Photoenhanced hydrogen insertion and transport in thiophene oligomers

M. BUNGS and H. TRIBUTSCH
Hahn-Meitner-Institut, Dept. Solare Energetik, 14109 Berlin, Germany
*(*author for correspondence)*

Received 6 October 1997; accepted in revised form 8 October 2001

Key words: ionics, IR-spectroscopy, photoelectro-chemistry, proton pumping, sexithiophene

Abstract

An electrochemical two-compartment cell was used to study the photo-induced insertion and transport of hydrogen through a palladium foil covered with a thin layer of the semiconducting thiophene oligomer sexithiophene, which photoelectrochemical current–voltage measurements have characterized as p-type with a photopotential of 200 mV and photocurrents up to 0.3 mA cm^{-2} at −0.8 V vs. SCE in a pH 3 electrolyte. Upon illumination the flux of hydrogen through the composite electrode was found to increase by a factor of two. The photoinduced enhancement on the hydrogen insertion was not stable since the photoactivity of the material altered under the influence of light. FTIR measurements showed that this is due to hydration of CC-double bonds destroying the conjunctive system of the p-orbitals necessary for the semiconducting properties. Diffusion coefficients of the sexithiophene/palladium electrode were found to be one order of magnitude smaller than in uncovered palladium, which was attributed to the lower hydrogen absorption in the oligomer. The relevance of light induced proton transfer in organic layers for the development of energy converting devices and sensors is discussed.

1. Introduction

Light induced proton transport is well known from biological systems. Examples are proton transport in thylacoide membranes during photosynthesis or light induced proton pumping across the membranes of halobacterium halobium. Photoinduced proton pumping is an essential mechanism in biological solar energy conversion. Artificial systems for solar energy conversion based on photoinduced ion transport reactions are presently not available but the scientific background and possible applications of light induced ionic processes have been discussed [1]. Due to the molecular variability of polymeric materials, these should be especially interesting model systems for attempts to convert light into electrochemical energy via ionic processes. Since semiconducting polymers combine photoconductive properties with the ability to electrochemically insert a variety of guest species, they appear to meet the basic requirements for such mechanisms. A first interesting example has already been investigated. It is the material poly(2,5)-furylen into which protons were inserted via a cathodic photoreaction [2]. Through such a photon induced insertion reaction, the free energy of the polymer electrode was changed which could be demonstrated by designing an energy storing solar cell. In the present work, efforts in the direction of protonic energy conversion systems are continued using thiophene oligomer layers. The purpose of this work is to construct a model system, which is able to convert light energy into a proton current across a polymer layer. Sexithiophene was selected as a polymer because it has been studied intensively with respect to photoelectric properties [3–10]. However, in all these studies photoinduced electron conduction has been investigated. In contrast, photon induced proton conduction is to be investigated in this work. This means, via appropriate mechanisms and barriers, proton movements will selectively be induced and monitored. The complete mechanism to be studied is consequently the conversion of light into proton movement and a protonic photopotential. This work aims at basic understanding of phenomena towards protonic photovoltaics [11].

2. Experimental

2.1. *Electrochemical cell and principle of measurement*

The intercalation experiments were carried out in a two-compartment cell, which allows the working electrode to be monitored independently in two electrochemical circuits. The two electrochemical cells were separated by the working electrode and each compartment was fitted with a platinum counter electrode and a calomel reference electrode. To allow illumination one side of the cell was equipped with a quartz window. Details are given in the block diagram of Figure 1.

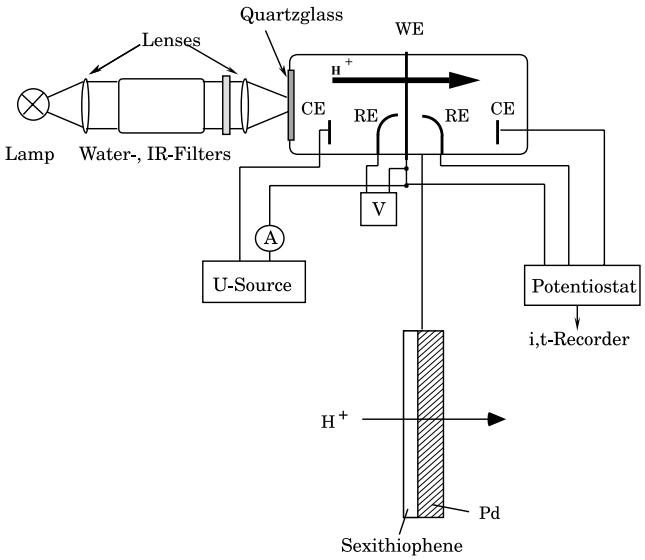

Fig. 1. Block-diagram of the electrochemical double cell. The working electrode consists of a palladium foil, which is covered with the oligomer on the left side. The direction of the proton flux through the cell is indicated by the arrow.

When a cathodic current or a negative potential is applied on one side hydrogen is intercalated and diffuses through the electrode. On the backside of the electrode the hydrogen release into the electrolyte is detectable by setting a suitable positive potential and recording the resulting oxidation current. This experimental technique was originally introduced by Frumkin and Aladzhalova [12] for the determination of hydrogen diffusion coefficients in metals. The transient current can be described on the basis of Fick's law. In our experiments potentiostatic conditions were chosen for both sides; thus, from the solution of the relevant differential equation the following expression for the transient current results [13]:

$$i_s(t) = i_\infty \left[1 + 2 \sum_{n=1}^{\infty} (-1)^n \exp\left(-\frac{n^2 \pi^2 D t}{s^2} \right) \right] \qquad (1)$$

where s, i, D, and t are electrode thickness, transient saturation current, diffusion coefficient, and time, respectively. To determine the diffusion coefficient two relations can be derived from Equation 1:

$$t_b = 0.5 \frac{s^2}{\pi^2 D} \qquad (2a)$$

$$t_L = \frac{1}{6} \frac{s^2}{D} \qquad (2b)$$

t_b, the break-through time, can be understood as the time that the first protons need to reach the backside of the electrode. The time lag t_L corresponds to the time required to reach a constant hydrogen concentration profile in the electrode [14] and is obtained from the intercept of the linear part of the integration curve of Equation 1. Thus the diffusion coefficient D for hydrogen may be obtained.

2.2. *Electrode, electrolytes and electrochemical conditions*

As electrodes foils of palladium (Aldrich, 99.9% purity, thickness 25 μm) covered on one side with a sexithiophene layer of 400-nm thickness were used. The sexithiophene was synthesized based on the method of Kagan and Arora [15] by a one-step procedure from terthiophene [16] and was made available to us from the CNRS, Thiaís. It consists of six thiophene units, which are interconnected via the 2,5-carbon atoms and was applied on the metal substrate by evaporation under vacuum. The electrode area exposed to the electrolyte was 0.78 cm^2. A pH 3 buffered solution (Merck) and a solution of 0.1 M Na_2SO_4 were used as electrolytes on the sexithiophene-covered side and the backside of the electrode respectively. Hydrogen intercalation experiments were performed under N_2-conditions using a glove box where the oxygen concentration was about 20 ppm.

For photoelectrochemical investigations smaller pieces of the sexithiophene covered metal foils (0.2 cm^2) were pasted on brass electrode holders, insulated with Scotch cast and cycled potentiodynamically in pH 3 and Eu(II)-solutions. To obtain Eu(II) an electrolyte of 0.02 M $EuCl_3$/KCl was prepared and a negative potential of -0.8 V was applied to an inserted Pb-electrode. A light intensity of 100 mW m^{-2} was chosen.

Hydrogen intercalation experiments where performed with potentials between -0.5 and -0.8 V vs. SCE at the sexithiophene side and 0.6 V vs. SCE at the backside of the electrodes.

3. Results and discussion

In Figure 2a and b the results of the photoelectrochemical measurements in a potential range between 0.2 and -1 V vs. SCE are displayed. In the dark the cathodic current is small with respect to the photocurrent. As can be expected from a p-type semiconductor there is a significant cathodic photocurrent reaching up to 0.8 mA cm^{-2} accompanied by a photopotential of 420 mV. The capacitive currents are small in the whole potential range indicating a very homogeneous character of the electrode surface. Cyclic voltammogramms in pH 3 electrolytes show a behavior which is similar, in principle, with the exception that photopotentials and photocurrents reach maximum values of 200 mV and 0.3 mA cm^{-2} respectively. After cycling multiple times under illumination H_2-bubbles were found at the electrode surface indicating that, in the absence of other redox species, protons serve as electron acceptors. A further difference between these two kinds of electrolyte is observed if one compares the stability of the photoactivity. Whereas photocurrent and photopotential remain stable in Eu(II)-solutions the photoactivity in pure pH 3 electrolytes is altered within a few cycles. This is best seen in the photoaction spectra inserted in Figure 2. Since the electrodes do not recover, these effects must be due to irreversible changes in the electrode material, e.g.

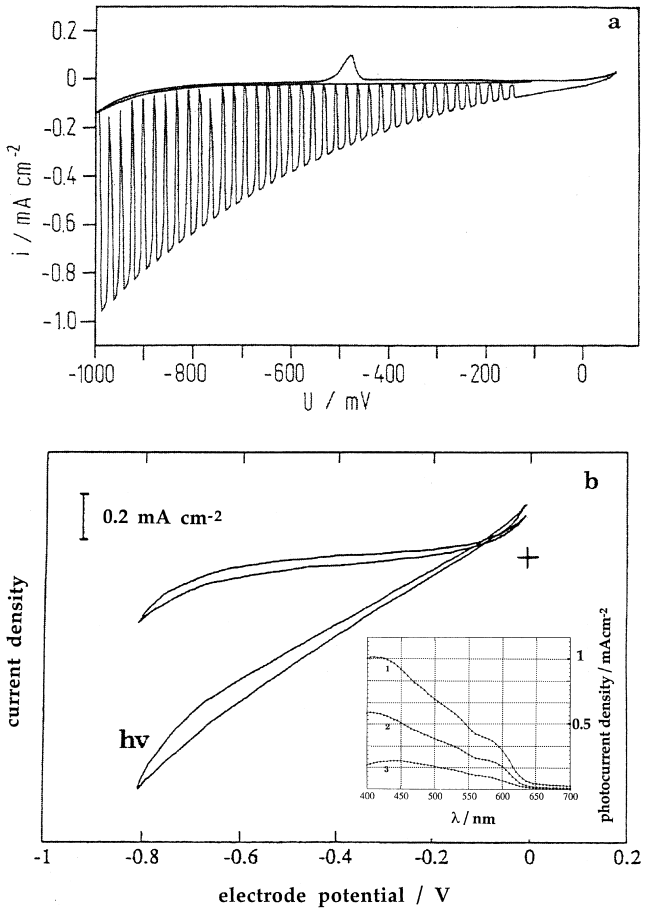

Fig. 2. Cyclic voltammetric behavior of sexithiophene in the dark and under illumination in (a) Eu(II)-electrolyte with chopped light; and (b) in pH 3 electrolyte. Scanrate: 20 mV s^{-1}. Inset: Photocurrent spectra in UV–Vis. with pH 3 electrolyte at a potential of −0.9 V. 1, 2 and 3 are spectra in intervals of 30 min showing the decay of photoactivity.

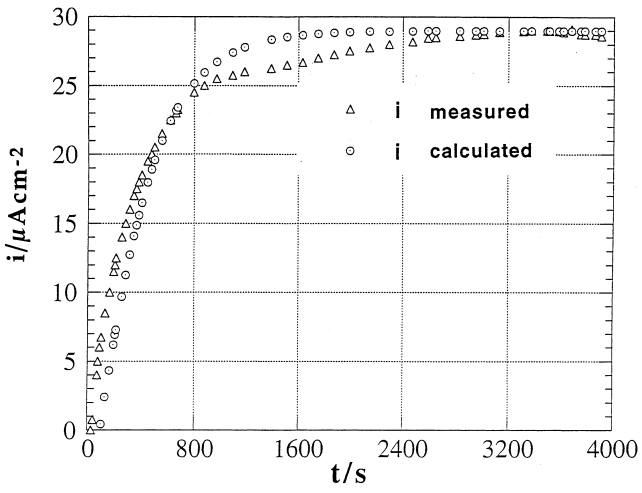

Fig. 3. The transient current at the backside of the sexithienyl/palladium composite electrode is proportional to hydrogen flux through the electrode.

Table 1. Diffusion coefficients of the composite sexithiophene/palladium electrode as obtained according to Equation 2a and b and of uncovered palladium (Pd_{blank})

6T/Pd	D (cm^2 s^{-1})
t_L	3×10^{-9}
t_b	2×10^{-8}
Pd_{blank}	0.9×10^{-7}

chemical processes in sexithiophene causing the deterioration of its semiconducting properties.

A typical evolution of the transient oxidation current for a non-illuminated electrode, where the potential on the sexithiophene covered side was adjusted at −0.8 V, is given in Figure 3. The ascent of the oxidation current started about 15 s after the potential on the entrance side was switched on. The permeation rate (P), i.e. the ratio between the transient saturation current (i_∞) and the corresponding reduction current on the hydrogen entrance side, was 0.7, thus indicating loss reactions. Diffusion coefficients, as derived from the breakthrough time and the time lag, are given in Table 1. It can be seen that the diffusion coefficients for the composite electrode, $D_{6T/Pd}$, are about one order of magnitude smaller compared to D_{Pd}. To interpret these results it has to be considered that the electrode consists of two layers with extremely different thickness and that the time lag in a multi-layer depends on the solubility for hydrogen and the diffusion coefficients in the individual layers [17]. Since the sexithiophene layer is only 0.3 μm compared to 25 μm of the Pd-foil neither a very fast nor a particular slow diffusion of hydrogen in the oligomer could explain the results in Table 1 if equal solubility is assumed. In the first case $D_{6T/Pd}$ only could reach $\approx D_{Pd}$, in the second case values for t_L and t_b would result which do not fit the experimental data. Therefore it has to be concluded that the lower diffusion coefficient $D_{6T/Pd}$ of the composite electrode is due to different hydrogen storage capacities in sexithiophene and palladium respectively.

Upon illumination the transient current is significantly increased starting after a retention time of 15 s. The increase is depending on the potential adjusted at the sexithiophene side of the electrode. At low negative potentials where the photocurrent of the oligomer is small the effect on the transient is also moderate, e.g. at −0.5 V the increase is only 5% whereas at a potential of −0.8 V the transient current is doubled (Figure 3a). The permeation rate remains unchanged. Since the experiments are potentiostatically controlled, this shows that the growth of the transient is caused by the photocurrent of sexithiophene, which adds to the cathodic dark current on the intercalation side.

On the other hand the photoactivity of the material is not very stable as observed already in the photoelectrochemical investigations. These changes were also found in the diffusion experiments and caused a fast decay of the photoinduced effect on the transient current. At the same time the transient current for the non-illuminated electrode decreased and the saturation current tended to become lower in a series of

measurements. After subsequent experiments with a hydrogen flux and a turnover of charge of 500 mC the photo effect was clearly diminished (Figure 3b). The color of the sexithiophene changed from orange-red to a pale yellow. Obviously chemical reactions occur parallel with the diffusion process, which alter the semiconducting properties of the material.

To investigate the nature of these side reactions FTIR spectra of juvenile samples were compared with the electrodes subjected to hydrogen intercalation experiments. The corresponding spectra are displayed in Figure 4a and b. Table 2 contains the vibrations of sexithiophene and their attribution based on investigations of different heterocyclic oligomers and polymers [9].

The difference between samples which are subjected to hydrogen intercalation and untreated ones, respectively, are the appearance of additional bands and changes in the intensity distribution of others. The latter is detectable more clearly if one forms the differential spectra by subtraction (not shown here). However, it can be observed that the γ-C—H-peak at 796 cm^{-1} is smaller and that the ν-C=C at 1493 cm^{-1} is bigger, a tendency which seems to be connected with the hydrogen flux.

Additional bands are observed at 2848 and 2924 cm^{-1} and correspond to symmetrical and asymmetrical stretching vibrations of aliphatic —C—H in $—CH_2$-groups. This indicates that C=C-double bonds of the oligomer become hydrogenated by the diffusing hydrogen. ν-C—C-bands, which would be expected in this case, should be found around 1000 cm^{-1} and can be assumed in the shoulder at 1020 cm^{-1}.

Table 2. IR vibrations of sexithiophene and their attribution

Wavenumber (cm^{-1})	Attribution
694	γ-C—H, at 2-substituted rings, out of plane
796	γ-C—H, at 2.5-substituted rings, out of plane
833	γ-C—H, out of plane
1063	δ-C—H, in plane
1425–1443	ν-C=C, symmetric
1493	ν-C=C, asymmetric
3063	ν-C—H, in β-position

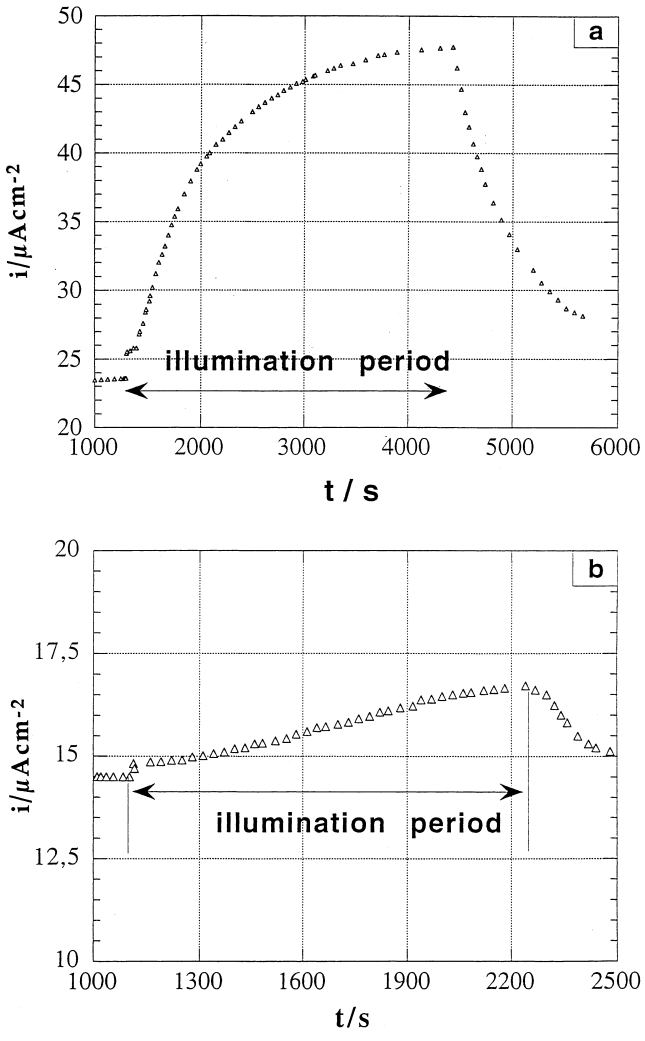

Fig. 4. Development of the transient current (a) on the backside of the sexithiophene/palladium composite electrode under illumination of the oligomer covered side; and (b) after a hydrogen flux corresponding to a charge of 500 mC.

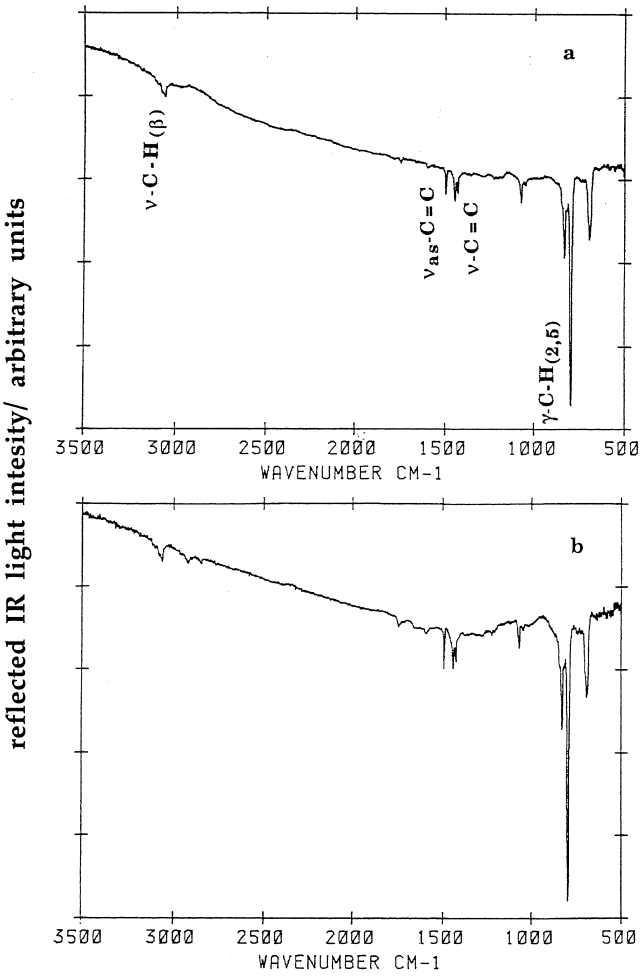

Fig. 5. FTIR reflection spectra of sexithiophene (a) on the palladium substrate; and (b) after multiple hydrogen diffusion experiments.

Following Furukawa et al. [19] the intensity ratio of symmetrical and asymmetrical ν-C=C bands should decrease with increasing chain length of thiophene oligomers. Since the intensity of ν-C=C$_{(as)}$ at 1493 cm^{-1} increased one might assume dimerization of two sexithienyl units or fragments. On the other hand the intensity of the γ-C—H-band could be interpreted as a decrease of 2.5 substituted rings. Since a dimerization reaction needs a suitable geometrical arrangement of molecules and C can be considered as immobilized on the electrode, a simple hydrogenation of C=C-double bonds which can occur anywhere in the carbon framework is more likely.

However, the most important result of the FTIR measurement (Figure 5) is that there is a hydrogenation reaction which obviously occurs parallel to proton diffusion and which causes the destruction of the conjugated π-bond system. Since the integrity of the π-system is necessary for the semiconducting properties, and hence for the photoactivity, photoinduced intercalation processes must come to an end if this condition is not fulfilled.

4. Conclusion

The experimental results demonstrate that it is possible to use the photoactivity of organic materials to enhance hydrogen insertion processes. With a composite sexithiophene/palladium electrode the hydrogen flux could be doubled under illumination. This means that photon powered proton pumps can, in principle, be operated with thin polymer layers. On the other hand, illumination in combination with proton transport through organic materials can cause hydrogenation reactions which damage the conjunctive π-bond-system, as is the case with sexithiophene. The mechanism of hydrogenation, the interaction of the quite reactive inserted atomic hydrogen species with the polymer π-bond-system is a chemical challenge, which has to be investigated carefully. Stable or stabilized organic layers have to be identified, before realistic advances towards light sensitive proton pumping organic membranes can be expected.

Acknowledgements

The authors would like to thank Dr D. Fichou for the sexithiophene samples and Dr Garnier for the opportunity for one of us (M.B.) to visit the CNRS-laboratory in Thiaís.

References

1. G. Betz and H. Tributsch, *Progr. Solid State Chem.* **16** (1985) 195.
2. G. Betz and H. Tributsch, *Solid State Ionics* **28–30** (1988) 1197.
3. G. Horowitz, F. Kouki and P. Valat, *Phys. Rev. B* **59** (1999) 10 651.
4. C. Botta, S. Destri, W. Porzio, A. Borghesi, A. Sassella, R. Tubino, G. Bongiovanni, M.A. Loi and A. Mura, *Phys. Rev. B* **60** (1999) 6039.
5. J.M. Maud, D. Herzberg, L. Hu, A.J. Salih and J.M. Marshall, *Synth. Met.* **102** (1998) 985.
6. G. Lanzani, G. Cerullo, S. Stagira, S. De Silvestri and F. Garnier, *Phys. Rev. B* **58** (1998) 7740.
7. M.J. Loiacono, E.L. Granstrom and C.D. Frisbie, *J. Phys. Chem. B* **102** (1998) 1679.
8. J.C. Wittmann, C. Straupe, S. Meyer, B. Lotz, P. Lang, G. Horowitz and F. Garnier, *Thin Solid Films* **333** (1998) 272.
9. S.C. Veenstra, G.G. Malliaras, H.J. Brouwer, F.J. Esselink, V.V. Krasnikov, P.F. Van Hutten, J. Wildeman, H.T. Jonkman, G.A. Sawatzky and G. Hadziioannou, *Synth. Met.* **84** (1997) 971.
10. S.C. Veenstra, G.G. Malliaras, H.J. Brouwer, F.J. Esselink, V.V. Krasnikov, P.F. Van Hutten, J. Wildeman, H.T. Jonkman, G.A. Sawatzky and G. Hadziioannou, *Proc. SPIE* **2852** (1996) 277.
11. H. Tributsch, *Ionics* **6** (2000) 16.
12. A.N. Frumkin and N.A. Aladzhalova, *Acta Phys. Chim. USSR* **19** (1944) 1.
13. J. Crank, 'The Mathematics of Diffusion' (Clarendon Press, London, 1975).
14. M.A.V. Devanathan and Z. Stachursky, *Proc. Roy. Soc. (London)* **270A** (1962) 90.
15. J. Kagan and S.K. Aroro, *Macromolecules* **20** (1983) 1937.
16. D. Fichou, G. Horowitz, Y. Nishikitani and F. Garnier, *Chemtronics* **3** (1988) 176.
17. J.A. Barrie, J.D. Levine, A.S. Michaels and P. Wong, *Trans. Faraday Soc.* **59** (1963) 869; R. Ash, R.M. Barrer and D.G. Palmer, *Br. J. Appl. Phys.* **16** (1965) 873.
18. A. Berlin, G.A. Pagani and F. Sannicolo, *Synth. Met.* **18** (1987) 157; S. Hasoon, M. Galtier, J.L. Sauvajol, J.P. Lere-Porte, A. Bonniol and B. Moukala, *Synth. Met.* **28** (1989) 1C317.
19. Y. Furukawa, M. Akimoto and I. Harada, *Synth. Met.* **18** (1987) 151.